Neurobiology of Aging 39 (2016) 99–107

Contents lists available at ScienceDirect

Neurobiology of Aging

journal homepage: www.elsevier.com/locate/neuaging

Acceleration of hippocampal atrophy rates in asymptomatic amyloidosis

K. Abigail Andrews [a,b], Chris Frost [a,c], Marc Modat [a,b], M. Jorge Cardoso [a,b], AIBL, Chris C. Rowe [d], Victor Villemagne [d], Nick C. Fox [a], Sebastien Ourselin [a,b], Jonathan M. Schott [a,*]

[a] Dementia Research Centre, Department of Neurodegenerative Disease, UCL Institute of Neurology, London, UK
[b] Centre for Medical Image Computing, UCL, London, UK
[c] London School of Hygiene and Tropical Medicine, London, UK
[d] Department of Nuclear Medicine and Centre for PET, Austin Health, Heidelberg, Victoria, Australia

ARTICLE INFO

Article history:
Received 8 May 2015
Received in revised form 9 September 2015
Accepted 14 October 2015
Available online 22 October 2015

Keywords:
Asymptomatic amyloidosis
Hippocampus
Atrophy
Acceleration
MRI
PET

ABSTRACT

Increased rates of brain atrophy measured from serial magnetic resonance imaging precede symptom onset in Alzheimer's disease and may be useful outcome measures for prodromal clinical trials. Appropriate trial design requires a detailed understanding of the relationships between β-amyloid load and accumulation, and rate of brain change at this stage of the disease. Fifty-two healthy individuals (72.3 ± 6.9 years) from Australian Imaging, Biomarkers and Lifestyle Study of Aging had serial (0, 18 m, 36 m) magnetic resonance imaging, (0, 18 m) Pittsburgh compound B positron emission tomography, and clinical assessments. We calculated rates of whole brain and hippocampal atrophy, ventricular enlargement, amyloid accumulation, and cognitive decline. Over 3 years, rates of whole brain atrophy ($p < 0.001$), left and right hippocampal atrophy ($p = 0.001$, $p = 0.023$), and ventricular expansion ($p < 0.001$) were associated with baseline β-amyloid load. Whole brain atrophy rates were also independently associated with β-amyloid accumulation over the first 18 months ($p = 0.003$). Acceleration of left hippocampal atrophy rate was associated with baseline β-amyloid load across the cohort ($p < 0.02$). We provide evidence that rates of atrophy are associated with both baseline β-amyloid load and accumulation, and that there is presymptomatic, amyloid-mediated acceleration of hippocampal atrophy. Clinical trials using rate of hippocampal atrophy as an outcome measure should not assume linear decline in the presymptomatic phase.

1. Introduction

Beta-amyloid (Aβ) deposition is one of the key hallmarks of Alzheimer's disease (Braak and Braak, 1997) and, according to the amyloid cascade hypothesis (Hardy and Selkoe, 2002), is a prime mover in the sequence of events leading to neurodegeneration and cognitive decline. The emergence of cerebrospinal fluid (CSF) measures of Aβ (Blennow and Hampel, 2003; Palmert et al., 1990) and positron emission tomography (PET) using ligands that bind to fibrillar amyloid deposits (Clark et al., 2011; Klunk et al., 2004) allow for Aβ deposition to be quantified in life. This in turn has led not only to the development of new, and potentially more specific criteria for the diagnosis of Alzheimer's disease incorporating biomarker evidence for Aβ deposition (Dubois et al., 2007, 2014; Jack et al., 2011a; McKhann et al., 2011), but also to fundamental changes in how we conceptualize Alzheimer's disease pathogenesis. The finding that approximately one-third of apparently healthy people in their 70s have significant levels of brain Aβ as determined using CSF (Shaw et al., 2009) or PET (Bourgeat et al., 2010; Jack et al., 2008a; Pike et al., 2007; Rowe et al., 2010) complements similar findings from autopsy studies (Knopman et al., 2003; Price and Morris, 1999), and has led to the definition of asymptomatic amyloidosis as a potentially presymptomatic Alzheimer's disease state (Morris et al., 1996, 2005; Sperling et al., 2009, Dubois et al., 2010), now formalized in research diagnostic criteria (Sperling et al., 2011a).

Biomarker studies of both familial Alzheimer's disease (Bateman et al., 2012) and aging, mild cognitive impairment (MCI), and sporadic Alzheimer's disease (Jack et al., 2013; Villemagne et al., 2013) have provided evidence to suggest that, at least in vulnerable individuals, amyloid accumulation may lead to a cascade of events including network breakdown

* Corresponding author at: Dementia Research Centre, UCL Institute of Neurology, Queen Square, London WC1N 3NG, UK. Tel.:+ 44 20 3448 3553; fax: +44 20 7697 0314.
E-mail address: j.schott@ucl.ac.uk (J.M. Schott).

0197-4580/
http://dx.doi.org/10.1016/j.neurobiolaging.2015.10.013

(measured using task free functional magnetic resonance imaging [MRI]), neuronal destruction (reflected by elevation of CSF tau), and increased rates of brain atrophy (quantified using serial MRI) in vulnerable regions. Importantly, all these events are thought to precede the development of cognitive decline and symptoms by a decade or more in the case of Aβ accumulation, and several years in the case of excess atrophy rates, opening a potential window for secondary prevention studies aiming to prevent or delay the time to the development of cognitive impairment (Bateman et al., 2011; Desikan et al., 2012; Sperling et al., 2011b, 2014). Formalized and revised in a series of highly influential articles (Jack et al., 2010, 2011b, 2012, 2013), current hypotheses predict not only the sequence of changes occurring during the prodromal phase of Alzheimer's disease (Young et al., 2014) but also the trajectory of biomarker changes in this sequence, suggesting that the rate at which each biomarker becomes abnormal occurs in a sigmoidal fashion, that is, showing initial rapid acceleration followed by a period of linear increase, before decelerating toward a steady state as the biomarker in question becomes abnormal (Caroli and Frisoni, 2010; Sabuncu et al., 2011). If, as predicted, amyloid accumulation precedes increased rates of atrophy, it would be expected that rates of atrophy in regions sensitive to Alzheimer's disease pathology, for example, the medial temporal lobe (Braak and Braak, 1997) would be higher in amyloid-positive cognitively normal individuals than in those without Aβ deposition; and if biomarker changes do follow a sigmoidal trajectory, that acceleration in rates of atrophy in vulnerable regions would relate to amyloid deposition. If indeed there were acceleration in rates of atrophy in prodromal Alzheimer's disease (AD), this would have implications for clinical trials in asymptomatic amyloidosis. Such trials typically include rate of hippocampal atrophy as an outcome measure, with the premise that a disease-modifying therapy would slow rates of atrophy toward that of controls, and are often predicated on rates of atrophy following a linear trajectory.

In this study, using 3 time-point data from the Australian Imaging, Biomarkers and Lifestyle Study of Aging (AIBL) study, we aimed to investigate the dynamics of neurodegeneration in relationship to amyloid load and accumulation in asymptomatic elderly subjects. In particular, we aimed to determine (1) the relationship between absolute measures of amyloid load and rates of amyloid accumulation with rates of atrophy; (2) if, as predicted by current hypothetical models, there is acceleration of regional rates of atrophy in amyloid-positive individuals; and (3) if so, the impact that this acceleration might have on the design of trials in asymptomatic amyloidosis using rates of atrophy as outcome measures.

2. Methods

2.1. Subjects

We downloaded data from the AIBL study available on the Laboratory of Neuro Imaging database (http://www.loni.usc.edu/). We included subjects designated as healthy controls at baseline who had PiB ^{11}C PET scans at baseline and 18 months and 3T MRI volumetric scans at baseline, 18 months and 3 years. Details of the AIBL methodology have previously been reported (Ellis et al., 2009). Briefly, healthy controls ≥60 years old were recruited from the community, ~50% having subjective memory complaints (subjective cognitive impairment, SCI), and ~50% being *APOE ε4* carriers. All subjects underwent standardized clinical and neuropsychological examinations, including the Mini-Mental State Examination (MMSE), clinical dementia rating (CDR) scale, and tests of immediate and delayed logical memory. Subjects were assessed for the presence or absence of subjective cognitive impairment and underwent apolipoprotein E (APOE) genotyping. Austin Health Human Research Ethics Committee approved the study and subjects provided written informed consent.

2.2. Image acquisition

PiB-PET scans were acquired using an Allegro PET camera (Phillips Medical Systems, the Netherlands). A transmission scan was performed for attenuation correction. Participants received 370MBq ^{11}C-PiB over 1 minute, and a 20-minute acquisition (6 × 5-minute frames) in 3D-mode was performed beginning 50 minutes after injection. PET images were reconstructed using a 3D row-action maximum-likelihood algorithm. Summed images from the 50–70 minute time-frames were used in this study. Sagittal T1-weighted MRI brain scans were acquired using a 3D magnetization prepared rapid gradient echo sequence on a Siemens Trio Tim 3T scanner, with 1 × 1 mm in-plane resolution; 1.2 mm slice thickness; repetition time/echo time/inversion time = 2300 ms/2.98 ms/900 ms; flip angle = 9°; field-of-view = 240 × 256; and 160 slices.

2.3. Image analysis

2.3.1. MRI volumes and atrophy rates

Images were corrected for intensity inhomogeneity using the N3 algorithm (Boyes et al., 2008) and whole brain segmentations produced at each time point using BrainMAPS (Leung et al., 2011). After 9-degrees-of-freedom registration of the follow-up to baseline scans and differential bias correction (Lewis and Fox, 2004), hippocampal segmentations were produced at each time point using HippoMAPS (Leung et al., 2010a). Each segmentation underwent a visual quality control process, with minimal manual editing where necessary. Ventricular volumes were delineated semi-automatically using the MIDAS software package (Evans et al., 2010). Volume change over time (mL) was calculated for ventricles (Schott et al., 2010a), hippocampi (Leung et al., 2010a), and whole brain (Leung et al., 2010b) using the boundary shift integral. Baseline total intracranial volume (TIV) was estimated using the FreeSurfer (http://surfer.nmr.mgh.harvard.edu/) image analysis suite v4.5.0 (Buckner et al., 2004).

2.3.2. Amyloid PET processing

MRI and PET images were processed as previously described (Andrews et al., 2013) to calculate mean neocortical PiB uptake. Briefly, the MRI were segmented into tissue classes using NiftySeg (Cardoso et al., 2011) and into regions of interest by registration with NiftyReg (Modat et al., 2010) to the Hammers 30-subject atlas set (Hammers et al., 2003) followed by label fusion with MultiSTEPS (Cardoso et al., 2013). The gray matter segmentation was combined with a subset of regions of interest (frontal, temporal, parietal and occipital lobes plus insula and cingulate cortex) to create a neocortical mask. The PET image was rigidly registered to the corresponding MRI and normalized by the mean cerebellar gray matter uptake to produce standardized uptake value ratios (SUVRs). Mean neocortical SUVR was then calculated in PET space as the robust fractional-volume-weighted mean under the neocortical mask.

2.4. Statistical methods

For the purposes of understanding the relationship between amyloid load, amyloid accumulation, atrophy rates, and cognitive scores, analyses were performed on the whole cohort. Although likely to have lower statistical power than analyses treating amyloid load as continuous, for the purposes of considering the design of future clinical trials, we additionally dichotomized individuals as

amyloid positive and/or negative using a baseline SUVR of 1.4 as previously described (Andrews et al., 2013).

2.4.1. Cross-sectional analyses

We used unpaired *t* tests (allowing for unequal variances) to compare mean ages between the amyloid-positive and -negative groups. Fisher's exact test was used to compare APOE ε4-positive proportions between these groups. Paired *t* tests were used to test hippocampal asymmetry within these groups, with an unpaired *t* test used to compare the extent of the asymmetry between the groups. Baseline brain volumes were compared between groups using generalized least squares regression models to adjust for potential effects of age, gender, and TIV. Generalized least squares models were used to allow the residual variance to differ in the 2 groups. An analogous model, but adjusting for age, gender, and (categorized) years of education was used to compare baseline cognitive scores.

2.4.2. Analysis of longitudinal change

The repeated longitudinal measures of cognition were analyzed using generalized least squares models to allow for potential differences in variance between groups and between time points and in the correlations between the various pairs of repeated measures. Models assumed unstructured covariance matrices for the repeated measures at the 3 time points with the variances and correlations between pairs of measurements separately estimated in the amyloid-positive and -negative groups. Models assumed linear rates of change in each group with covariates such as age, gender, and education allowed to influence both absolute levels and rates of change.

The repeated longitudinal measures of change in brain volumes were also analyzed using generalized least squares models. Models assumed unstructured covariance matrices for the 2 measures of change with the variances and correlations between pairs of measurements separately estimated in the amyloid-positive and -negative groups. Models assumed linear rates of change in each group with covariates such as age, gender, and TIV allowed to influence rates of change. Furthermore, models assessed acceleration by incorporating quadratic effects of time and with the extent of the acceleration allowed to depend on covariates. One set of models treated amyloid load as a continuous variable, whilst a second set dichotomized the subjects into 2 groups as mentioned previously.

2.4.3. Sample size estimates for trials

To explore the influence of the dynamics of longitudinal change in atrophy rates on clinical trial design, we used data from amyloid-positive individuals to estimate required sample sizes for clinical trials that provide 80% power, 5% type-1 error, to detect a 25% absolute reduction in whole brain, ventricular, and hippocampal change over each 18-month period, and over 36 months. Bias-corrected and accelerated 95% bootstrap (100,000 samples) confidence intervals (Efron and Tibshirani, 1994) were found for required sample size estimates and for ratios of such estimates (analyzed on a logarithmic scale). Analyses were performed in Stata13 (Stata Corp, TX).

3. Results

3.1. Demographics and baseline characteristics

Complete data for 53 individuals were available. One individual who had progressed to non-AD dementia was excluded. Twenty-three of 52 (44%) were male, mean (±SD) age was 72.3 ± 6.9 years, baseline MMSE was 29.2 ± 1.2, 15/52 (29%) were APOE ε4 positive, 12/52 (23%) had SCI, 49/52 had a CDR = 0, the remaining 3 had a CDR of 0.5, and 13/52 (25%) were amyloid positive at a cutoff SUVR = 1.4. Amyloid-positive individuals were slightly older but not significantly so (74.3 vs. 71.6; $p = 0.17$) but were more likely to be APOE ε4 positive (61.5% vs. 18.0%; $p = 0.005$). Fifty were classified as "normal control" at all 3 time points; one individual was reclassified as "MCI" at 18 months and "Alzheimer's disease" at 36 months, another as "Alzheimer's disease" at both 18 months and 36 months.

Cognitive scores, amyloid load (global cortical SUVR), and global and regional volumes at baseline are shown in Table 1 for the whole cohort, and for amyloid-positive and -negative groups. In the cohort, as a whole, there was statistically significant (right > left) hippocampal asymmetry ($p < 0.0001$), with no evidence ($p = 0.4$) that the extent of the asymmetry differed between the amyloid-positive and -negative individuals. There was no evidence that the cognitive scores differed between the amyloid-positive and -negative groups. Although unadjusted mean brain volumes were similar in the amyloid-positive and -negative groups, after adjustment for age, gender, and TIV whole brain volumes were on average 30 mL (95% CI 2–57 mL, $p = 0.037$) smaller in the amyloid-positive group compared with the negative group, this largely being a consequence of the fact that the mean TIV in the amyloid-positive group was somewhat larger than that in the negative group. Ventricular and hippocampal volumes were similar in the 2 groups.

3.2. Longitudinal changes over 36 months

3.2.1. Changes in cognition and amyloid load

Table 2 shows the mean and standard deviation of rates of change in cognitive outcomes and in SUVR in the amyloid-positive

Table 1
Cognitive scores, SUVR, and brain volumes at baseline

	All individuals (n = 52)		Amyloid positive (SUVR > 1.4; n = 13)		Amyloid negative (SUVR < 1.4; n = 39)		Comparison amyloid positive versus negative
	Mean	SD	Mean	SD	Mean	SD	Adjusted[a] mean difference (95% CI)
SUVR	1.33	0.32	1.82	0.29	1.17	0.06	—
MMSE	29.2	1.2	29.2	1.2	29.1	1.2	0.4 (−0.2, 1.1)
Logical memory immediate recall	13.1	4.0	12.2	3.8	13.4	4.0	−1.1 (−3.6, 1.4)
Logical memory delayed recall	11.9 (2)	4.1	11.8 (1)	3.7	11.9 (1)	4.2	0.2 (−2.5, 2.9)
Total intracranial volume (mL)	1509	149	1552	148	1494	149	—
Brain volume (mL)	1088	94	1086	91	1089	97	**−30 (−57, −2)**
Ventricular volume (mL)	35.0	19.6	38.0	22.9	34.0	18.6	−1.1 (−13.2, 10.9)
Left hippocampal volume (mL)	2.62	0.37	2.65	0.45	2.61	0.35	0.07 (−0.19, 0.33)
Right hippocampal volume (mL)	2.74	0.37	2.74	0.46	2.73	0.34	−0.00 (−0.27, 0.26)

Numbers in brackets are numbers of missing observations.
Statistically significant ($p < 0.05$) results are shown in bold.
Key: MMSE, Mini-Mental State Examination; SUVR, standardized uptake value ratio.
[a] Comparisons made after adjustment for age, gender and total intracranial volume (imaging outcomes) and age, gender, and education (others).

Table 2
Comparison of rates of change over each time period for selected variables

	0–18 m, mean ± SD	18–36 m, mean ± SD	Mean rate[a] (95% confidence interval)	Acceleration/yr[b] (95% confidence interval)
Amyloid positive (SUVR > 1.4; n = 13)				
Consecutive scan interval (d)	545 ± 89	579 ± 64	—	—
Increase in SUVR (SUVR/yr)	0.024 ± 0.053	—	—	—
Change in MMSE/y	−0.9 ± 0.9	0.1 ± 0.8	**−0.4 (−0.7, −0.1)**	—
Change in logical memory immediate/y	0.2 ± 2.4	−0.7 ± 2.9	−0.4 (−1.3, 0.5)	
Change in logical memory delayed/y	0.0 ± 3.2	−0.5 ± 2.6	−0.6 (−1.1, 0.0)	
Brain atrophy (mL/y)	5.6 ± 5.2	9.1 ± 5.9	**7.1 (5.4, 8.8)**	2.7 (−0.6, 5.9)
Ventricular expansion (mL/y)	1.8 ± 1.4	2.4 ± 1.9	**2.0 (1.2, 2.8)**	0.4 (−0.1, 0.8)
Left hippocampal atrophy (μL/y)	17 ± 28	48 ± 39	**27 (14, 41)**	**24 (8, 40)**
Right hippocampal atrophy (μL/y)	18 ± 24	37 ± 38	**18 (4, 31)**	**13 (0, 25)**
Amyloid negative (SUVR < 1.4; n = 39)				
Consecutive scan interval (d)	551 ± 97	592 ± 70	—	—
Increase in SUVR (SUVR/y)	0.007 ± 0.025	—	—	—
Change in MMSE/y	−0.1 ± 0.9	0.0 ± 0.8	−0.0 (−0.2, 0.1)	—
Change in logical memory immediate/y	0.2 ± 2.5	−0.1 ± 2.0	−0.0 (−0.4, 0.4)	—
Change in logical memory delayed/yr	0.6 ± 2.9	−0.1 ± 1.7	0.2 (−0.2, 0.5)	—
Brain atrophy (mL/y)	4.3 ± 5.3	3.1 ± 3.9	**3.6 (2.7, 4.5)**	−0.3 (−1.7, 1.0)
Ventricular expansion (mL/y)	1.0 ± 0.9	1.2 ± 1.1	**1.1 (0.8, 1.3)**	0.1 (−0.1, 0.3)
Left hippocampal atrophy (μL/y)	9 ± 24	15 ± 22	**12 (8, 17)**	6 (−1, 12)
Right hippocampal atrophy (μL/y)	7 ± 31	10 ± 26	**8 (3, 13)**	6 (−2, 14)

Key: MMSE, Mini-Mental State Examination; SUVR, standardized uptake value ratio.
[a] Derived from a generalized least squares regression model (see statistical methods) where the rate of change is assumed constant over the 2 periods. Statistically significant ($p < 0.05$) results (where the 95% confidence interval does not span 0) are shown in bold.
[b] Derived from a generalized least squares regression model (see statistical methods) where the rate of change over the 2 periods is assumed to change at a constant rate. The acceleration is the change in rate over 1 year. Statistically significant ($p < 0.05$) results are shown in bold.

and -negative groups in the 2 follow-up periods. On average, over the 36 month period, MMSE scores declined in the amyloid-positive group with a mean rate of change of 0.4/y (95% CI 0.1–0.7 mL/y, $p = 0.015$). Directionally similar changes were seen for the other 2 cognitive measures with that for delayed logical memory being of borderline statistical significance ($p = 0.055$). In contrast, there was little or no mean change in the amyloid-negative group, with both the mean MMSE rate of change ($p = 0.021$) and the rate of change in the delayed logical memory test ($p = 0.029$) differing significantly from the analogous rates in the amyloid-positive group after adjusting for age, gender, and years of education.

The mean rate of change in SUVR between baseline and 18 months was 0.01 per year (95% CI 0.001–0.02, $p = 0.026$) across the whole cohort. The mean rate in those who were amyloid positive at baseline was around 3 times that in those who were amyloid negative, although this difference was not statistically significant ($p = 0.13$).

3.2.2. Relating rates of volume change over 36 months to amyloid load

Fig. 1 plots the subject specific annualized rates of change in whole brain, ventricular, and left and right hippocampal volumes against baseline amyloid load in the 2 time periods. From the repeated measures generalized least squares regression models, higher baseline amyloid load was significantly associated with increased rates of whole brain atrophy ($p < 0.001$), ventricular expansion ($p < 0.001$), and left ($p = 0.001$) and right hippocampal atrophy rates ($p = 0.023$) after adjustment for age, gender, and TIV. These associations were little altered and remained statistically significant (all $p < 0.01$) after additionally adjusting simultaneously for years of education, MMSE, CDR, SCI, and APOE ε4 status.

Extending the regression models described previously to simultaneously investigate the effects of baseline amyloid load and rate of amyloid accumulation on rates (adjusting for effects of age, gender, and TIV) provided some evidence of an independent effect of amyloid accumulation. Specifically, for whole brain atrophy rate, there was statistically significant evidence ($p = 0.003$) that an increased rate of accumulation was associated with increased atrophy. For ventricular expansion, and both left and right hippocampal atrophy rates, directionally consistent results were seen with borderline statistically significant p-values (between 0.063 and 0.101).

3.2.3. Comparing volume changes in amyloid-positive and -negative groups

Table 2 shows the mean and standard deviation rates of volume change in the amyloid-positive and -negative groups together with estimated mean rates of change and 95% CI. All mean rates of atrophy were markedly higher in the amyloid-positive group, with rates of whole brain atrophy and ventricular expansion approximately double, and hippocampal atrophy measures more than double those in the amyloid-negative group.

3.3. Longitudinal changes over 0–18 and 18–36 month intervals

3.3.1. Acceleration in atrophy rates

Table 2 also shows estimates of acceleration in atrophy rates estimated from linear mixed models that allowed the rate of atrophy to change with time. In the amyloid-positive group, rates of left and right hippocampal atrophy in the second 18-month period were more than double those seen in the first, this acceleration being statistically significant ($p < 0.05$) for both structures. Results for rates of whole brain atrophy and ventricular expansion were also suggestive of acceleration, although these effects were not statistically significant. In the amyloid-negative group, both hippocampal atrophy rates were somewhat higher in the second 18-month period than the first although the size of the difference was markedly smaller than that for the amyloid-positive group and not statistically significant. Comparisons of hippocampal acceleration between the 2 groups (adjusting for age, gender, and TIV) did not give statistically significant results, although results for the left hippocampus were borderline statistically significant ($p = 0.058$). Furthermore, an analysis that treated amyloid load as a continuous variable did provide statistically significant evidence that the acceleration in left hippocampal atrophy rate was associated with amyloid load ($p = 0.018$).

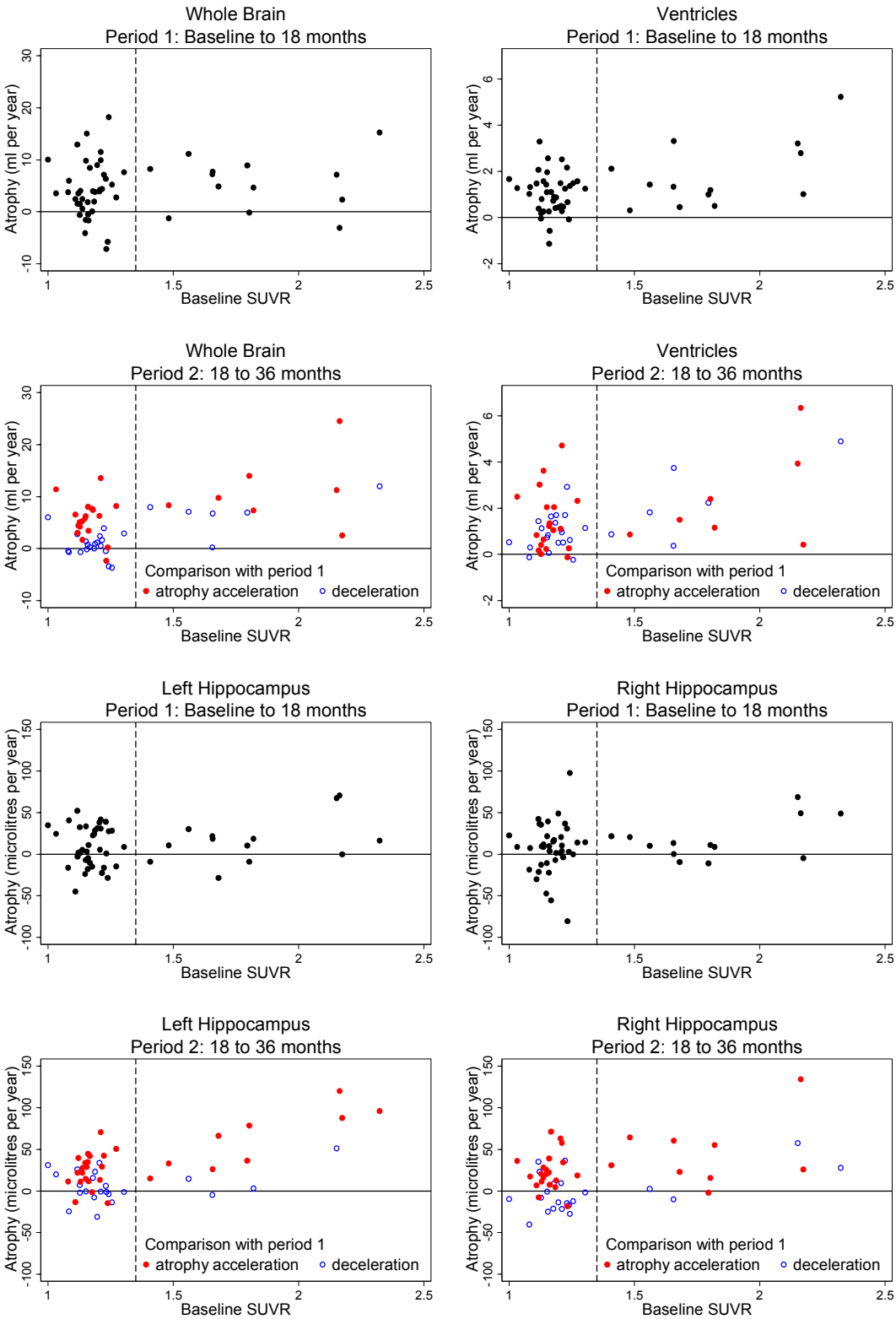

Fig. 1. Atrophy rates by period and region. In panels showing rates in period 2 closed triangles (red closed circles in the web version) indicate that the rate was greater than that in period 1 whilst open squares (blue open circles in the web version) indicate the converse.

3.3.2. *Sample size estimates*

Recruiting amyloid-positive subjects to power a 3-year treatment trial to detect 25% per year absolute slowing of cerebral atrophy rates requires 44 (95% CI 20–96) subjects per arm using whole brain atrophy, 139 (84–232) using ventricular expansion, 161 (89–359) using left hippocampal atrophy rates, and 271 (129–788) using right hippocampal atrophy rates. Comparing sample size estimates across the 2 available 18 month time periods, numbers estimated to detect a 25% absolute reduction in rate of ventricular expansion were very similar, although with wide 95%

confidence intervals: 153 (86–332) and 157 (87–324) over 0–18 m and 18–36 m, respectively. However, for the other measures of atrophy, there were considerable, albeit nonsignificant (as assessed by consideration of confidence intervals on ratios of sample size estimates), reductions in numbers needed between the 2 time periods: for whole brain atrophy rates reductions were from 211 (70–1148) to 105 (43–304) per arm, whilst for rates of left and right hippocampal atrophy reductions were from 701 (206–61,824) to 164 (77–426) per arm and from 490 (182–3645) to 261 (114–875) per arm, respectively.

4. Discussion

In this study, we confirm an independent relationship between baseline amyloid load and rates of neurodegeneration over 36 months, provide evidence that atrophy rates are also influenced by the rate of amyloid accumulation in the first 18-month period, and show that these relationships are largely driven by individuals who are initially amyloid positive. We provide evidence that, as predicted by current hypotheses, asymptomatic amyloid-positive individuals, but not amyloid-negative individuals, show acceleration in rates of hippocampal atrophy. Finally, we demonstrate that sample sizes for clinical trials in asymptomatic amyloidosis based on rates of brain atrophy are dependent not only on the "length" of the trial, but particularly in the case of hippocampal atrophy, on the "timing" of a putative trial, with some evidence that smaller numbers are required closer to predicted disease onset. Importantly, this has implications for clinical trial design in prodromal disease, demonstrating that whilst it may be reasonable to assume linear change over longer periods, trials over shorter periods or adopting run-in designs cannot assume a consistent linear rate of decline.

The relationship between amyloid deposition and rates of atrophy has been investigated in a number of studies. Whereas some failed to determine a relationship between amyloid load and global cortical gray matter atrophy in asymptomatic individuals (Storandt et al., 2012), our finding that baseline amyloid burden—independent of age, APOE status, or cognition—independently influences rates of brain atrophy, hippocampal atrophy, and ventricular expansion in asymptomatic elderly individuals confirms and extends our previous findings over shorter intervals (Andrews et al., 2013; Schott et al., 2010b) and those of others (Chételat et al., 2012; Scheinin et al., 2009). Taken together with the finding that atrophy rates are associated not only with baseline amyloid load but also with rate of amyloid accumulation, confirming findings from a previous report (Villemagne et al., 2013), this provides strong evidence not only for a close link between the presence of significant brain amyloid and downstream neurodegeneration but also suggests that there is also a dynamic element with "on-going" amyloid accumulation influencing rate of neurodegeneration. This in turn suggests that strategies to prevent further amyloid accumulation may impact on rate of neurodegeneration, and perhaps the emergence of symptoms, even if the neurodegenerative process has already been initiated.

Our finding of acceleration of rate of hippocampal atrophy in the amyloid-positive group, with trends for acceleration in measures of whole brain change, is consistent with current models of AD pathogenesis, which predict both that increased rates of atrophy within medial temporal structures occurs before increase in more global atrophy measures (Jack et al., 2010; Schott et al., 2003; Whitwell et al., 2007; Young et al., 2014), but also that the rate of change is sigmoidal—that is, associated with an initial period of acceleration (Caroli and Frisoni, 2010; Jack et al., 2013; Schuff et al., 2012). This suggests that acceleration of atrophy starts both some time after the build-up of significant amyloid load, and at least 18 months before symptom onset, in keeping with the current model of biomarker progression (Jack et al., 2013). Several longitudinal studies have demonstrated acceleration of brain atrophy in symptomatic familial Alzheimer's disease (Chan et al., 2003; Ridha et al., 2006), and sporadic MCI or Alzheimer's disease (Jack et al., 2008b; Leung et al., 2013; Schuff et al., 2009). Carlson and colleagues reported that rates of ventricular enlargement in healthy controls increased more than 2 years before the emergence of clinical cognitive impairment (Carlson et al., 2008). Sabuncu and colleagues reported acceleration of cortical thinning and hippocampal loss in the early stages of the disease, measured over 3 time points in the course of 1 year (Sabuncu et al., 2011), but this acceleration, as in a number of the aforementioned studies, was calculated across the cohort relative to MMSE score, rather than on the basis of individual subject scans. Our results are, to the best of our knowledge, the first demonstration of within-subject, presymptomatic acceleration of hippocampal atrophy rates in amyloid-positive individuals. Moreover, by using a methodology for calculating rates of change that has been, and continues to be, used in clinical trials, our data can be used to explore the effect that this acceleration might have on sample sizes for similar trials.

Although increased rates of atrophy in relation to baseline amyloid load, and acceleration of hippocampal atrophy, were seen across the group as a whole, these results were predominantly driven by those individuals with asymptomatic amyloidosis. Mean rates of whole brain, hippocampal atrophy, and ventricular expansion were very similar in both 18-month periods in the amyloid-negative group. By contrast, in the amyloid-positive group, hippocampal atrophy was approximately 2-3 fold higher in the second 18 months compared to the first, with whole brain atrophy approximately doubling, and rate of ventricular expansion also increasing. For clinical trials, particularly for rates of hippocampal change, the increase in mean rate of change in the second 18-month time period results in somewhat reduced sample size estimates during this period. It should be noted that whilst the sample sizes presented here are relatively small, they are based on absolute reductions of 25%. Assuming that drug treatment would at most reduce rates of atrophy to those of the amyloid-negative group this equates to a treatment effect of 48% for whole brain, 53% for ventricles, and 38% for hippocampi.

Independent of the absolute sample size estimates which are based on relatively small numbers, the demonstration of acceleration in rates of hippocampal atrophy and its effects on sample sizes has more general implications for the design of disease-modifying trials using rates of atrophy as outcome measures in asymptomatic amyloidosis. As sample sizes are critically dependent not only on the absolute extent of change but also on the standard deviation of the observed change, it is not surprising that smaller sample sizes are required for trials over 36 compared to 18 months. The demonstration of acceleration of atrophy between 2 successive 18-month intervals suggests that over shorter periods it may be not only the length of the trial, but the "proximity" to symptom onset that will influence required sample sizes. It follows that run-in trial designs, which depend on extrapolation of rate of change from an initial period off-treatment to that on the study drug, may not be able to assume the same rate of linear decline between both periods at least in the presymptomatic phase; and there are likely to be similar caveats for cross-over trials at this stage of the disease.

This study has a number of limitations. The study period extends only over 36 months and 3 time points precluding a more fine-grained assessment of the dynamics of biomarker change. The number of individuals in the study is relatively small, meaning that considerable caution is required when interpreting the sample size estimates for clinical trials, which require further replication in larger groups, are best considered indicative, and are based on the premise that treatment will attenuate rates of atrophy. We note that

the rates of hippocampal atrophy presented here over the first 18 months are somewhat lower than we have previous reported from a slightly larger sample of this cohort (n = 66) (Andrews et al., 2013). Excluded individuals had either not attended for a third MRI or had not had a second amyloid PET scan. A higher proportion of missing individuals were amyloid positive (9/22) than amyloid negative (4/44). Although none of the amyloid-negative missing individuals had left the study at the third time point, more than half (5/9) of the amyloid-positive group had. Of those missing, 3 with particularly high rates of atrophy included one who had converted to a diagnosis of "other dementia", another who had converted to MCI, whereas the third had not been available for assessment at the third time point. These results demonstrate the suggestion that individuals dropping out of clinical trials, even at the asymptomatic stage, should not be assumed to be missing completely at random (Schott and Bartlett, 2012).

5. Conclusions

These results clearly distinguish between levels and dynamics of rates in "healthy" normal aging and in asymptomatic amyloidosis, being consistent both with the initial upswing in atrophy rates described by the sigmoidal curves proposed in Jack et al. (2010) and investigated in further longitudinal studies (Caroli and Frisoni, 2010; Jack et al., 2013; Sabuncu et al., 2011; Schuff et al., 2012) and with a sequence of events whereby amyloid accumulation leads to acceleration of downstream neurodegeneration and cognitive decline, consistent with the proposed model of disease progression. Using methodologies currently in use in clinical trials, we demonstrate that rate of accumulation of amyloid as well as absolute level of deposited fibrillar amyloid influence rates of atrophy, suggesting that strategies to slow amyloid accumulation as opposed to promoting clearance may also be beneficial. The demonstration that hippocampal atrophy rates accelerate before symptom onset in amyloid-positive individuals suggests that clinical trial design in asymptomatic amyloidosis should not assume linear rates of biomarker progression.

Disclosure statement

NF has provided consultancy to GE Healthcare, Janssen-Cilag, Janssen-Elan pharmaceuticals, AVID Radiopharmaceuticals Inc, Lilly Research Labs, Eisai Inc and Johnson & Johnson; JS receives grant funding from AVID Radiopharmaceuticals Inc, receives royalties from Henry Stewart talks, and has consulted for Eli Lilly and Roche. CR has received research grants for imaging in dementia from Avid Radiopharmaceuticals, GE Healthcare, Piramal Imaging, Astra Zeneca and Navidea Biopharmaceuticals. He has been a consultant or paid speaker at sponsored conference sessions for Piramal, GE Healthcare, Astra Zeneca, Roche and Janssen. All other authors confirm that they have no competing interests to disclose.

Acknowledgements

Data used in the preparation of this article was obtained from the Australian Imaging Biomarkers and Lifestyle flagship study of ageing (AIBL) which was made available at the ADNI database (www.loni.usc.edu/ADNI). This work was supported by the National Institute for Health Research (NIHR) Queen Square Biomedical Research Unit in Dementia and the UCL/H Biomedical Research Center, and we gratefully acknowledge the support of the Leonard Wolfson Experimental Neurology Centre. The Dementia Research Centre (DRC) is an Alzheimer's Research UK (ARUK) Coordinating Centre and has also received equipment funded by ARUK (www.alzheimersresearchuk.org). For providing the data for this study, the authors thank the AIBL Study Group (www.aibl.csiro.au) which is supported by the Commonwealth Scientific Industrial Research Organization (CSIRO) Flagship Collaboration Fund through the Australian Imaging, Biomarkers and Lifestyle (AIBL) Flagship study of Ageing, the Austin Hospital Medical Research Foundation, Neurosciences Victoria, and the University of Melbourne; we also thank the AIBL participants and their carers for their valuable contribution. K. Abigail Andrews is funded by an EPSRC (www.epsrc.ac.uk) PhD studentship. Sebastien Ourselin receives funding from the EPSRC (EP/H046410/1, EP/J020990/1, EP/K005278), the MRC (MR/J01107X/1), the EU-FP7 project VPH-DARE@IT (FP7-ICT-2011-9-601055), the NIHR Biomedical Research Unit (Dementia) at UCL and the National Institute for Health Research University College London Hospitals Biomedical Research Centre (NIHR BRC UCLH/UCL High Impact Initiative- BW.mn.BRC10269); Marc Modat is supported by the UCL Leonard Wolfson Experimental Neurology Centre (PR/ylr/18575); Nick C. Fox is an NIHR Senior Scientist and also holds grants from the National Institute on Aging (NIH) USA (5U01AG024904-10) for work on ADNI. Jonathan M. Schott receives grant funding from ARUK (ARUK-PG2014-1946) and the MRC Dementias Platform UK (MR/L023784/1 and MR/009076/1), and acknowledges the support of the UCL/H Biomedical Research Centre. The funders had no role in study design, data collection and analysis, decision to publish, or preparation of the article.

References

Andrews, K.A., Modat, M., Macdonald, K.E., Yeatman, T., Cardoso, M.J., Leung, K.K., Barnes, J., Villemagne, V.L., Rowe, C.C., Fox, N.C., Ourselin, S., Schott, J.M., 2013. Atrophy rates in asymptomatic amyloidosis: implications for Alzheimer prevention trials. PLoS One 8, e58816.

Bateman, R.J., Aisen, P.S., De Strooper, B., Fox, N.C., Lemere, C.A., Ringman, J.M., Salloway, S., Sperling, R.A., Windisch, M., Xiong, C., 2011. Autosomal-dominant Alzheimer's disease: a review and proposal for the prevention of Alzheimer's disease. Alzheimers. Res. Ther. 3, 1.

Bateman, R.J., Xiong, C., Benzinger, T.L.S., Fagan, A.M., Goate, A., Fox, N.C., Marcus, D.S., Cairns, N.J., Xie, X., Blazey, T.M., Holtzman, D.M., Santacruz, A., Buckles, V., Oliver, A., Moulder, K., Aisen, P.S., Ghetti, B., Klunk, W.E., McDade, E., Martins, R.N., Masters, C.L., Mayeux, R., Ringman, J.M., Rossor, M.N., Schofield, P.R., Sperling, R.A., Salloway, S., Morris, J.C., 2012. Clinical and biomarker changes in dominantly inherited Alzheimer's disease. N. Engl. J. Med. 367, 795–804.

Blennow, K., Hampel, H., 2003. CSF markers for incipient Alzheimer's disease. Lancet Neurol. 2, 605–613.

Bourgeat, P., Chételat, G., Villemagne, V.L., Fripp, J., Raniga, P., Pike, K., Acosta, O., Szoeke, C., Ourselin, S., Ames, D., Ellis, K.A., Martins, R.N., Masters, C.L., Rowe, C.C., Salvado, O., 2010. Beta-amyloid burden in the temporal neocortex is related to hippocampal atrophy in elderly subjects without dementia. Neurology 74, 121–127.

Boyes, R.G., Gunter, J.L., Frost, C., Janke, A.L., Yeatman, T., Hill, D.L.G., Bernstein, M.A., Thompson, P.M., Weiner, M.W., Schuff, N., Alexander, G.E., Killiany, R.J., DeCarli, C., Jack, C.R., Fox, N.C., 2008. Intensity non-uniformity correction using N3 on 3-T scanners with multichannel phased array coils. Neuroimage 39, 1752–1762.

Braak, H., Braak, E., 1997. Frequency of stages of Alzheimer-related lesions in different age categories. Neurobiol. Aging 18, 351–357.

Buckner, R.L., Head, D., Parker, J., Fotenos, A.F., Marcus, D., Morris, J.C., Snyder, A.Z., 2004. A unified approach for morphometric and functional data analysis in young, old, and demented adults using automated atlas-based head size normalization: reliability and validation against manual measurement of total intracranial volume. Neuroimage 23, 724–738.

Cardoso, M.J., Clarkson, M.J., Ridgway, G.R., Modat, M., Fox, N.C., Ourselin, S., 2011. LoAd: a locally adaptive cortical segmentation algorithm. Neuroimage 56, 1386–1397.

Cardoso, M.J., Leung, K., Modat, M., Keihaninejad, S., Cash, D., Barnes, J., Fox, N.C., Ourselin, S., 2013. STEPS: Similarity and Truth Estimation for Propagated Segmentations and its application to hippocampal segmentation and brain parcelation. Med. Image Anal 17, 671–684.

Carlson, N.E., Moore, M.M., Dame, A., Howieson, D., Silbert, L.C., Quinn, J.F., Kaye, J.A., 2008. Trajectories of brain loss in aging and the development of cognitive impairment. Neurology 70, 828–833.

Caroli, A., Frisoni, G.B., 2010. The dynamics of Alzheimer's disease biomarkers in the Alzheimer's Disease Neuroimaging Initiative cohort. Neurobiol. Aging 31, 1263–1274.

Chan, D., Janssen, J.C., Whitwell, J.L., Watt, H.C., Jenkins, R., Frost, C., Rossor, M.N., Fox, N.C., 2003. Change in rates of cerebral atrophy over time in early-onset Alzheimer's disease: longitudinal MRI study. Lancet 362, 1121–1122.

Chételat, G., Villemagne, V.L., Villain, N., Jones, G., Ellis, K.A., Ames, D., Martins, R.N., Masters, C.L., Rowe, C.C., 2012. Accelerated cortical atrophy in cognitively normal elderly with high β-amyloid deposition. Neurology 78, 477–484.

Clark, C.M., Schneider, J.A., Bedell, B.J., Beach, T.G., Bilker, W.B., Mintun, M.A., Pontecorvo, M.J., Hefti, F., Carpenter, A.P., Flitter, M.L., Krautkramer, M.J., Kung, H.F., Coleman, R.E., Doraiswamy, P.M., Fleisher, A.S., Sabbagh, M.N., Sadowsky, C.H., Reiman, E.P., Reiman, P.E.M., Zehntner, S.P., Skovronsky, D.M., 2011. Use of florbetapir-PET for imaging beta-amyloid pathology. JAMA 305, 275–283.

Desikan, R.S., McEvoy, L.K., Thompson, W.K., Holland, D., Brewer, J.B., Aisen, P.S., Aisen, P.S., Sperling, R.A., Dale, A.M., 2012. Amyloid-β–associated clinical decline occurs only in the presence of elevated P-tau. Arch. Neurol. 69, 709–713.

Dubois, B., Feldman, H.H., Jacova, C., Cummings, J.L., Dekosky, S.T., Barberger-Gateau, P., Delacourte, A., Frisoni, G., Fox, N.C., Galasko, D., Gauthier, S., Hampel, H., Jicha, G.A., Meguro, K., O'Brien, J., Pasquier, F., Robert, P., Rossor, M., Salloway, S., Sarazin, M., de Souza, L.C., Stern, Y., Visser, P.J., Scheltens, P., 2010. Revising the definition of Alzheimer's disease: a new lexicon. Lancet Neurol. 9, 1118–1127.

Dubois, B., Feldman, H.H., Jacova, C., Dekosky, S.T., Barberger-Gateau, P., Cummings, J., Delacourte, A., Galasko, D., Gauthier, S., Jicha, G., Meguro, K., O'brien, J., Pasquier, F., Robert, P., Rossor, M., Salloway, S., Stern, Y., Visser, P.J., Scheltens, P., 2007. Research criteria for the diagnosis of Alzheimer's disease: revising the NINCDS-ADRDA criteria. Lancet Neurol. 6, 734–746.

Dubois, B., Feldman, H.H., Jacova, C., Hampel, H., Molinuevo, J.L., Blennow, K., DeKosky, S.T., Gauthier, S., Selkoe, D., Bateman, R., Cappa, S., Crutch, S., Engelborghs, S., Frisoni, G.B., Fox, N.C., Galasko, D., Habert, M.-O., Jicha, G.A., Nordberg, A., Pasquier, F., Rabinovici, G., Robert, P., Rowe, C., Salloway, S., Sarazin, M., Epelbaum, S., de Souza, L.C., Vellas, B., Visser, P.J., Schneider, L., Stern, Y., Scheltens, P., Cummings, J.L., 2014. Advancing research diagnostic criteria for Alzheimer's disease: the IWG-2 criteria. Lancet Neurol. 13, 614–629.

Efron, B., Tibshirani, R.J., 1994. An Introduction to the Bootstrap. Chapman & Hall/CRC, Boca Raton, London, New York, Washington DC.

Ellis, K.A., Bush, A.I., Darby, D., De Fazio, D., Foster, J., Hudson, P., Lautenschlager, N.T., Lenzo, N., Martins, R.N., Maruff, P., Masters, C., Milner, A., Pike, K., Rowe, C., Savage, G., Szoeke, C., Taddei, K., Villemagne, V., Woodward, M., Ames, D., 2009. The Australian Imaging, Biomarkers and Lifestyle (AIBL) study of aging: methodology and baseline characteristics of 1112 individuals recruited for a longitudinal study of Alzheimer's disease. Int. Psychogeriatr. 21, 672–687.

Evans, M.C., Barnes, J., Nielsen, C., Kim, L.G., Clegg, S.L., Blair, M., Leung, K.K., Douiri, A., Boyes, R.G., Ourselin, S., Fox, N.C., 2010. Volume changes in Alzheimer's disease and mild cognitive impairment: cognitive associations. Eur. Radiol. 20, 674–682.

Hammers, A., Allom, R., Koepp, M.J., Free, S.L., Myers, R., Lemieux, L., Mitchell, T.N., Brooks, D.J., Duncan, J.S., 2003. Three-dimensional maximum probability atlas of the human brain, with particular reference to the temporal lobe. Hum. Brain Mapp. 19, 224–247.

Hardy, J., Selkoe, D.J., 2002. The amyloid hypothesis of Alzheimer's disease: progress and problems on the road to therapeutics. Science 297, 353–356.

Jack, C.R., Albert, M.S., Knopman, D.S., McKhann, G.M., Sperling, R.A., Carrillo, M.C., Thies, B., Phelps, C.H., 2011a. Introduction to the recommendations from the National Institute on Aging-Alzheimer's Association workgroups on diagnostic guidelines for Alzheimer's disease. Alzheimers Dement. 7, 257–262.

Jack, C.R., Knopman, D.S., Jagust, W.J., Petersen, R.C., Weiner, M.W., Aisen, P.S., Shaw, L.M., Vemuri, P., Wiste, H.J., Weigand, S.D., Lesnick, T.G., Pankratz, V.S., Donohue, M.C., Trojanowski, J.Q., 2013. Tracking pathophysiological processes in Alzheimer's disease: an updated hypothetical model of dynamic biomarkers. Lancet Neurol. 12, 207–216.

Jack, C.R., Knopman, D.S., Jagust, W.J., Shaw, L.M., Aisen, P.S., Weiner, M.W., Petersen, R.C., Trojanowski, J.Q., 2010. Hypothetical model of dynamic biomarkers of the Alzheimer's pathological cascade. Lancet Neurol. 9, 119–128.

Jack, C.R., Lowe, V.J., Senjem, M.L., Weigand, S.D., Kemp, B.J., Shiung, M.M., Knopman, D.S., Boeve, B.F., Klunk, W.E., Mathis, C.A., Petersen, R.C., 2008a. 11C PiB and structural MRI provide complementary information in imaging of Alzheimer's disease and amnestic mild cognitive impairment. Brain 131, 665–680.

Jack, C.R., Vemuri, P., Wiste, H.J., Weigand, S.D., Aisen, P.S., Trojanowski, J.Q., Shaw, L.M., Bernstein, M.A., Petersen, R.C., Weiner, M.W., Knopman, D.S., 2011b. Evidence for ordering of Alzheimer disease biomarkers. Arch. Neurol. 68, 1526–1535.

Jack, C.R., Vemuri, P., Wiste, H.J., Weigand, S.D., Lesnick, T.G., Lowe, V., Kantarci, K., Bernstein, M.A., Senjem, M.L., Gunter, J.L., Boeve, B.F., Trojanowski, J.Q., Shaw, L.M., Aisen, P.S., Weiner, M.W., Petersen, R.C., Knopman, D.S., 2012. Shapes of the trajectories of 5 major biomarkers of Alzheimer disease. Arch. Neurol. 69, 856–867.

Jack, C.R., Weigand, S.D., Shiung, M.M., Przybelski, S.A., O'Brien, P.C., Gunter, J.L., Knopman, D.S., Boeve, B.F., Smith, G.E., Petersen, R.C., 2008b. Atrophy rates accelerate in amnestic mild cognitive impairment. Neurology 70, 1740–1752.

Klunk, W.E., Engler, H., Nordberg, A., Wang, Y., Blomqvist, G., Holt, D.P., Bergström, M., Savitcheva, I., Huang, G., Estrada, S., Ausén, B., Debnath, M.L., Barletta, J., Price, J.C., Sandell, J., Lopresti, B.J., Wall, A., Koivisto, P., Antoni, G., Mathis, C.A., Långström, B., 2004. Imaging brain amyloid in Alzheimer's disease with Pittsburgh Compound-B. Ann. Neurol. 55, 306–319.

Knopman, D.S., Parisi, J.E., Salviati, A., Floriach-Robert, M., Boeve, B.F., Ivnik, R.J., Smith, G.E., Dickson, D.W., Johnson, K.A., Petersen, L.E., McDonald, W.C., Braak, H., Petersen, R.C., 2003. Neuropathology of cognitively normal elderly. J. Neuropathol. Exp. Neurol. 62, 1087–1095.

Leung, K.K., Barnes, J., Modat, M., Ridgway, G.R., Bartlett, J.W., Fox, N.C., Ourselin, S., 2011. Brain MAPS: an automated, accurate and robust brain extraction technique using a template library. Neuroimage 55, 1091–1108.

Leung, K.K., Barnes, J., Ridgway, G.R., Bartlett, J.W., Clarkson, M.J., Macdonald, K., Schuff, N., Fox, N.C., Ourselin, S., 2010a. Automated cross-sectional and longitudinal hippocampal volume measurement in mild cognitive impairment and Alzheimer's disease. Neuroimage 51, 1345–1359.

Leung, K.K., Bartlett, J.W., Barnes, J., Manning, E.N., Ourselin, S., Fox, N.C., 2013. Cerebral atrophy in mild cognitive impairment and Alzheimer disease: rates and acceleration. Neurology 80, 648–654.

Leung, K.K., Clarkson, M.J., Bartlett, J.W., Clegg, S., Jack, C.R., Weiner, M.W., Fox, N.C., Ourselin, S., 2010b. Robust atrophy rate measurement in Alzheimer's disease using multi-site serial MRI: tissue-specific intensity normalization and parameter selection. Neuroimage 50, 516–523.

Lewis, E.B., Fox, N.C., 2004. Correction of differential intensity inhomogeneity in longitudinal MR images. Neuroimage 23, 75–83.

McKhann, G.M., Knopman, D.S., Chertkow, H., Hyman, B.T., Jack, C.R., Kawas, C.H., Klunk, W.E., Koroshetz, W.J., Manly, J.J., Mayeux, R., Mohs, R.C., Morris, J.C., Rossor, M.N., Scheltens, P., Carrillo, M.C., Thies, B., Weintraub, S., Phelps, C.H., 2011. The diagnosis of dementia due to Alzheimer's disease: recommendations from the National Institute on Aging-Alzheimer's Association workgroups on diagnostic guidelines for Alzheimer's disease. Alzheimers Dement. 7, 263–269.

Modat, M., Ridgway, G.R., Taylor, Z.A., Lehmann, M., Barnes, J., Hawkes, D.J., Fox, N.C., Ourselin, S., 2010. Fast free-form deformation using graphics processing units. Comput. Methods Programs Biomed. 98, 278–284.

Morris, J.C., Kimberly, A., Quaid, K., Holtzman, D.M., Kantarci, K., Kaye, J., Reiman, E.M., Klunk, W.E., Siemers, E.R., 2005. Role of biomarkers in studies of presymptomatic Alzheimer's disease. Alzheimers Dement. 1, 145–151.

Morris, J.C., Storandt, M., McKeel, D.W., Rubin, E.H., Price, J.L., Grant, E.A., Berg, L., 1996. Cerebral amyloid deposition and diffuse plaques in "normal" aging: evidence for presymptomatic and very mild Alzheimer's disease. Neurology 46, 707–719.

Palmert, M.R., Usiak, M., Mayeux, R., Raskind, M., Tourtellotte, W.W., Younkin, S.G., 1990. Soluble derivatives of the beta amyloid protein precursor in cerebrospinal fluid: alterations in normal aging and in Alzheimer's disease. Neurology 40, 1028–1034.

Pike, K.E., Savage, G., Villemagne, V.L., Ng, S., Moss, S.A., Maruff, P., Mathis, C.A., Klunk, W.E., Masters, C.L., Rowe, C.C., 2007. Beta-amyloid imaging and memory in non-demented individuals: evidence for preclinical Alzheimer's disease. Brain 130, 2837–2844.

Price, J.L., Morris, J.C., 1999. Tangles and plaques in nondemented aging and "preclinical" Alzheimer's disease. Ann. Neurol. 45, 358–368.

Ridha, B.H., Barnes, J., Bartlett, J.W., Godbolt, A., Pepple, T., Rossor, M.N., Fox, N.C., 2006. Tracking atrophy progression in familial Alzheimer's disease: a serial MRI study. Lancet Neurol. 5, 828–834.

Rowe, C.C., Ellis, K.A., Rimajova, M., Bourgeat, P., Pike, K.E., Jones, G., Fripp, J., Tochon-Danguy, H., Morandeau, L., O'Keefe, G., Price, R., Raniga, P., Robins, P., Acosta, O., Lenzo, N., Szoeke, C., Salvado, O., Head, R., Martins, R., Masters, C.L., Ames, D., Villemagne, V.L., 2010. Amyloid imaging results from the Australian Imaging, Biomarkers and Lifestyle (AIBL) study of aging. Neurobiol. Aging 31, 1275–1283.

Sabuncu, M.R., Desikan, R.S., Sepulcre, J., Yeo, B.T.T., Liu, H., Schmansky, N.J., Reuter, M., Weiner, M.W., Buckner, R.L., Sperling, R.A., Fischl, B., 2011. The dynamics of cortical and hippocampal atrophy in Alzheimer disease. Arch. Neurol. 68, 1040–1048.

Scheinin, N.M., Aalto, S., Koikkalainen, J., Lötjönen, J., Karrasch, M., Kemppainen, N., Viitanen, M., Nagren, K., Helin, S., Scheinin, M., Rinne, J.O., 2009. Follow-up of [11C]PIB uptake and brain volume in patients with Alzheimer disease and controls. Neurology 73, 1186–1192.

Schott, J.M., Bartlett, J.W., Barnes, J., Leung, K.K., Ourselin, S., Fox, N.C., 2010a. Reduced sample sizes for atrophy outcomes in Alzheimer's disease trials: baseline adjustment. Neurobiol. Aging 31, 1452–1462, 1462.e1–e2.

Schott, J.M., Bartlett, J.W., Fox, N.C., Barnes, J., 2010b. Increased brain atrophy rates in cognitively normal older adults with low cerebrospinal fluid Aβ1-42. Ann. Neurol. 68, 825–834.

Schott, J.M., Bartlett, J.W., 2012. Investigating missing data in Alzheimer disease studies. Neurology 78, 1370–1371.

Schott, J.M., Fox, N.C., Frost, C., Scahill, R.I., Janssen, J.C., Chan, D., Jenkins, R., Rossor, M.N., 2003. Assessing the onset of structural change in familial Alzheimer's disease. Ann. Neurol. 53, 181–188.

Schuff, N., Tosun, D., Insel, P.S., Chiang, G.C., Truran, D., Aisen, P.S., Jack, C.R., Weiner, M.W., 2012. Nonlinear time course of brain volume loss in cognitively normal and impaired elders. Neurobiol. Aging 33, 845–855.

Schuff, N., Woerner, N., Boreta, L., Kornfield, T., Shaw, L.M., Trojanowski, J.Q., Thompson, P.M., Jack, C.R., Weiner, M.W., 2009. MRI of hippocampal volume loss in early Alzheimer's disease in relation to ApoE genotype and biomarkers. Brain 132, 1067–1077.

Shaw, L.M., Vanderstichele, H., Knapik-Czajka, M., Clark, C.M., Aisen, P.S., Petersen, R.C., Blennow, K., Soares, H., Simon, A., Lewczuk, P., Dean, R., Siemers, E., Potter, W., Lee, V.M.-Y., Trojanowski, J.Q., 2009. Cerebrospinal fluid biomarker signature in Alzheimer's disease neuroimaging initiative subjects. Ann. Neurol. 65, 403–413.

Sperling, R.A., Aisen, P.S., Beckett, L.A., Bennett, D.A., Craft, S., Fagan, A.M., Iwatsubo, T., Jack, C.R., Kaye, J., Montine, T.J., Park, D.C., Reiman, E.M., Rowe, C.C., Siemers, E., Stern, Y., Yaffe, K., Carrillo, M.C., Thies, B., Morrison-Bogorad, M.,

Wagster, M.V., Phelps, C.H., 2011a. Toward defining the preclinical stages of Alzheimer' disease: recommendations from the National Institute on Aging-Alzheimer's Association workgroups on diagnostic guidelines for Alzheimer's disease. Alzheimers Dement. 7, 280–292.

Sperling, R.A., Jack, C.R., Aisen, P.S., 2011b. Testing the right target and right drug at the right stage. Sci. Transl. Med. 3, 111cm33.

Sperling, R.A., Laviolette, P.S., O'Keefe, K., O'Brien, J., Rentz, D.M., Pihlajamaki, M., Marshall, G., Hyman, B.T., Selkoe, D.J., Hedden, T., Buckner, R.L., Becker, J.A., Johnson, K.A., 2009. Amyloid deposition is associated with impaired default network function in older persons without dementia. Neuron 63, 178–188.

Sperling, R.A., Rentz, D.M., Johnson, K.A., Karlawish, J., Donohue, M., Salmon, D.P., Aisen, P., 2014. The A4 study: stopping AD before symptoms begin? Sci. Transl. Med. 6, 228fs13.

Storandt, M., Head, D., Fagan, A.M., Holtzman, D.M., Morris, J.C., 2012. Toward a multifactorial model of Alzheimer disease. Neurobiol. Aging 33, 2262–2271.

Villemagne, V.L., Burnham, S., Bourgeat, P., Brown, B., Ellis, K.A., Salvado, O., Szoeke, C., Macaulay, S.L., Martins, R., Maruff, P., Ames, D., Rowe, C.C., Masters, C.L., 2013. Amyloid β deposition, neurodegeneration, and cognitive decline in sporadic Alzheimer's disease: a prospective cohort study. Lancet Neurol. 12, 357–367.

Whitwell, J.L., Przybelski, S.A., Weigand, S.D., Knopman, D.S., Boeve, B.F., Petersen, R.C., Jack, C.R., 2007. 3D maps from multiple MRI illustrate changing atrophy patterns as subjects progress from mild cognitive impairment to Alzheimer's disease. Brain 130, 1777–1786.

Young, A.L., Oxtoby, N.P., Daga, P., Cash, D.M., Fox, N.C., Ourselin, S., Schott, J.M., Alexander, D.C., 2014. A data-driven model of biomarker changes in sporadic Alzheimer's disease. Brain 137, 2564–2577.